MitoFit Preprints 2024.2
https://doi.org/10.26124/mitofit:2024-0002

BEC Spotlight

Cite
Cardoso LHD, Gnaiger E (2024) OXPHOS coupling and uncoupling. MitoFit Preprints 2024.2. https://doi.org/10.26124/mitofit:2024-0002

Author contributions
Both authors contributed equally to this manuscript.

Conflicts of interest
EG holds the position of Editor-in-Chief for BEC and is blinded from reviewing or making decisions for the manuscript. LHDC holds the position of Co-Editor-in-Chief for BEC and is blinded from reviewing or making decisions for the manuscript.

Online 2024-04-24

OXPHOS coupling and uncoupling

Luiza H D Cardoso, Erich Gnaiger
Oroboros Instruments, Innsbruck, Austria
luiza.cardoso@oroboros.at, erich.gnaiger@oroboros.at

Summary

Coupling of OXPHOS is classically studied by comparing ADP-stimulated O_2 flux (OXPHOS capacity *P* at saturating ADP and P_i concentrations) with non-phosphorylating LEAK respiration *L*, maintained mainly to compensate for the proton leak at high chemiosmotic potential in mitochondrial preparations supplied with fuel substrates to support mitochondrial electron transfer. However, measurement of the non-coupled electron transfer capacity *E* (ET capacity at collapsed chemiosmotic potential) yields additional information on coupling, since ET capacity may exceed OXPHOS capacity.

Keywords - electron transfer capacity, LEAK respiration, mitochondria, oxidative phosphorylation

1. Respiratory states and rates

LEAK respiration is limited in the absence of oxidative phosphorylation and provides an estimate of the intrinsically uncoupled respiration, without experimentally added protonophore. *L* can be assessed (*1*) in isolated mitochondria after complete phosphorylation of ADP to ATP, *L*(T) or state 4 (Chance, Williams 1955), (*2*) in the absence of adenylates, *L*(n), prior to addition of ADP (Estabrook 1967), or (*3*) after inhibition of the phosphorylation system, e.g. after inhibition of ATP synthase with oligomycin, *L*(Omy), or inhibition of adenine nucleotide translocase with carboxyatractyloside, *L*(Cat), in mitochondrial preparations and living cells (Gnaiger et al 2020).

The extent of stimulation of respiration by ADP, from the LEAK to the OXPHOS state, is related to coupling of electron transfer to phosphorylation, since *L* is suppressed in direct proportion to the tightness of coupling in a given pathway state. Alternatively, protonophores, also called uncouplers, are applied to short-circuit the H^+ cycle across the mitochondrial inner membrane and thus stimulate respiration from the LEAK state to maximum respiration for assessing the electron transfer (ET) capacity in terms of oxygen consumption uncontrolled by phosphorylation of ADP (Figure 1). Equine muscle mitochondria have identical OXPHOS and ET capacity measured at physiological temperature (Davis et al 2020; 2024). How is this related to OXPHOS coupling?

2. Three coupling control steps

Stimulation of oxygen consumption by ADP or uncoupler provides identical estimates of coupling in cases when $E = P$ (Figure 1c). E cannot be lower than P, although experimental artefacts may cause inhibition of E below the level of P, most frequently by application of insufficient or excessive concentrations of uncoupler (Steinlechner-Maran et al 1996) or high concentration of oligomycin (Doerrier et al 2018; Zdrazilova et al 2022). ET capacity, however, is higher than OXPHOS capacity if the phosphorylation system capacity limits respiration in the OXPHOS state. In this case, the utilization of the protonmotive force exerts limitation of O_2 flux. This limitation is removed by protonophore titrations, revealing a higher capacity to generate the protonmotive force by the ET system (Figure 1a). The most accurate method to measure this excess capacity (E-P) is provided by adding ADP initially (P), and subsequent titrations of uncoupler (E). An absence of stimulation of respiration in this protocol must not be mistaken as an indication of intrinsic uncoupling of these mitochondria.

In cases where $E>P$, the expression LEAK respiration and ET capacity as the biochemical coupling efficiency (1-L/E) provides a higher and more accurate estimate of intrinsic uncoupling or dyscoupling, since the P-L control efficiency (1-L/P) is lowered by limited capacities of the phosphorylation system, unrelated to coupling (Figure 1b, d) (Gnaiger 2020).

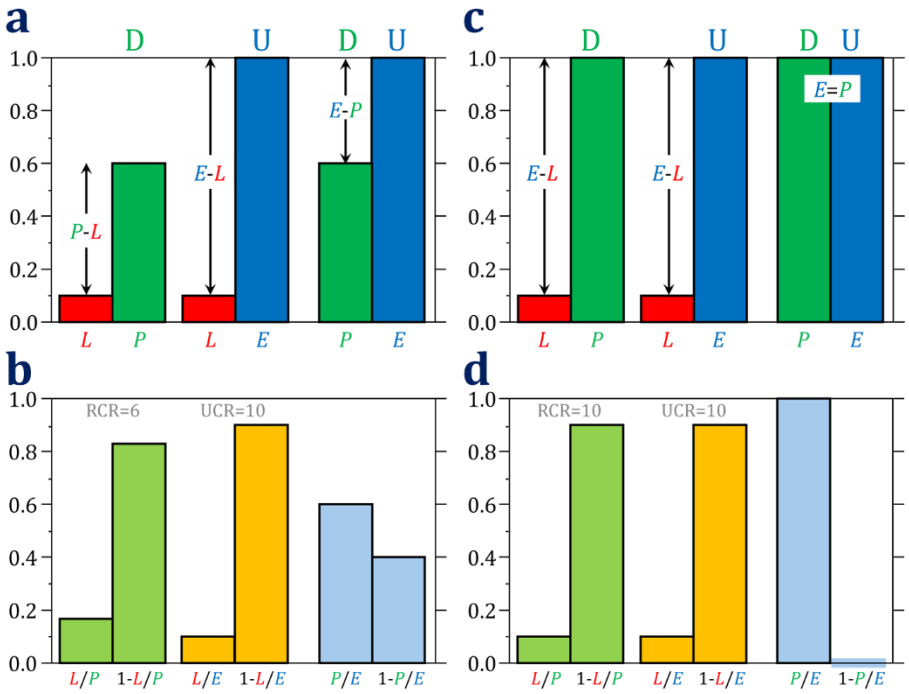

Figure 1: Three coupling control steps at a given pathway state in mitochondrial preparations, titrating (*1*) ADP (D) and (*2*) uncoupler (U) in the LEAK state or (*3*) uncoupler in the OXPHOS state. Corresponding coupling control parameters highlight the relationship between respiratory rates L, P, and E, in LEAK, OXPHOS, and ET states. **(a)** and **(b)** Mitochondria with $E>P$ and 1-P/E > 0. **(c)** and **(d)** Mitochondria with P=E and 1-P/E = 0. The P-L control efficiency is 1-L/P = (P-L)/P. The biochemical coupling efficiency is 1-L/E = (E-L)/E. The E-P control efficiency is 1-P/E = (E-P)/E (Gnaiger 2020). RCR = P/L; UCR = E/L.

3. Three mechanisms change the *E-P* excess capacity

When mitochondria with high *E-P* are observed to lose the *E-P* excess capacity, three alternative mechanisms must be distinguished: (*1*) Dyscoupling by increase of *L* and reduction of the biochemical coupling efficiency 1-*L*/*E*, which induces a higher *P* at constant *E*; (*2*) increase of phosphorylation system capacity increasing coupled *P* at constant *E* and *L*; and (*3*) decrease of electron transfer capacity *E* at constant *P* and *L* (Figure 2). Some experimental examples illustrate these mechanisms responsible for the decline of *E-P* control efficiency which may occur exclusively or in combination.

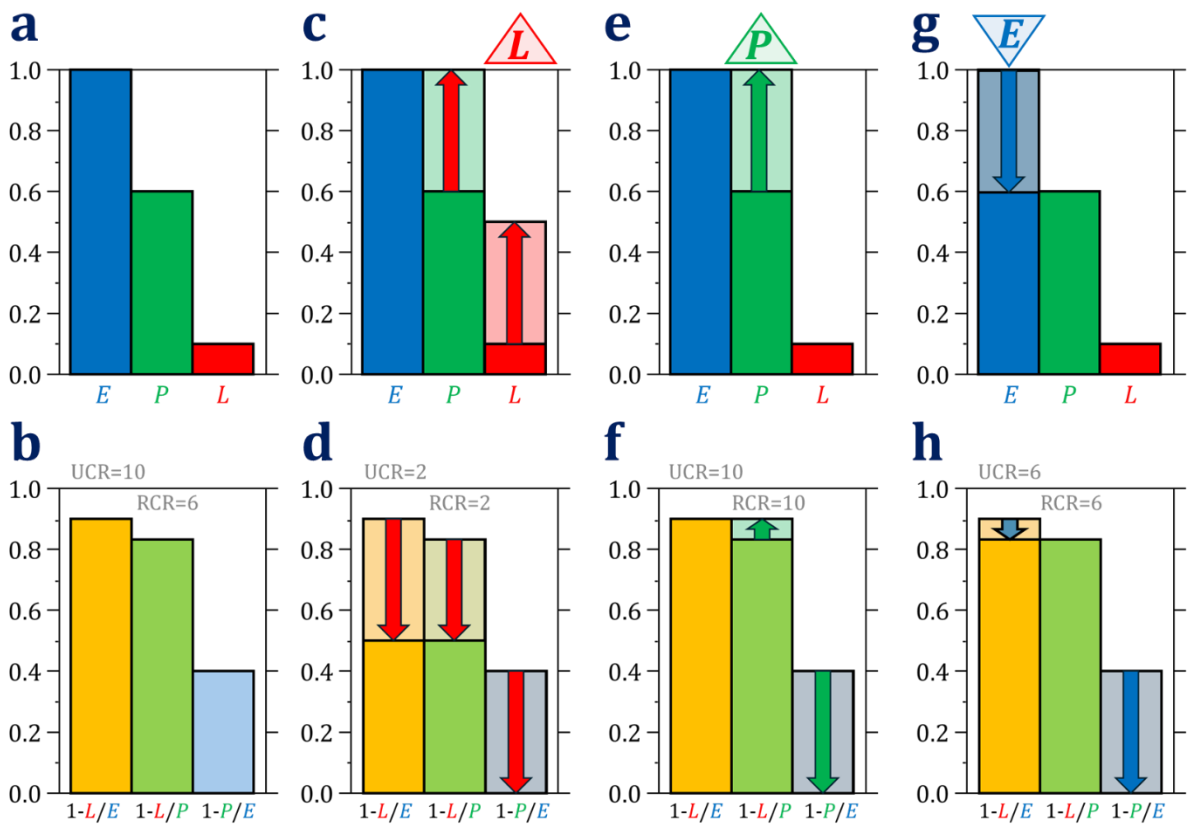

Figure 2: Different mechanisms that change coupling control in mitochondria at a given pathway state from *E*>*P* (**a** and **b**) to coupling control with *E*=*P* and thus loss of *E-P* excess capacity. **(c, d)** Dyscoupling with an increase of LEAK respiration *L* at constant *E*. **(e, f)** Increase of the phosphorylation system capacity leading to increased *P* at constant *E* and *L*. **(g, h)** Decrease of electron transfer capacity *E* at constant *P* and *L*.

During cold storage up to 9 h of human cardiac tissue, the *E-P* control efficiency (NS-pathway) decreases from 0.4 to zero at a cold storage time of 144 h (Lemieux et al 2011). At a first glance it appears paradoxical that the NADH-linked (N) pathway OXPHOS capacity (N_P) increased in response to the stress of cold storage, since a higher OXPHOS capacity may be interpreted as a positive outcome. However, rather than a higher capacity of phosphorylation, dyscoupling caused an increase of *P*, evidenced by the increase of *L*, while *E* remained constant (Lemieux et al 2011). Therefore, the loss of *E-P* control efficiency was caused by dyscoupling (Figure 2c, d).

Ten-weeks strength and endurance training of sedentary males induces a decrease of the *E-P* control efficiency (fatty acid oxidation, NADH and succinate-liked pathways,

FNS-pathway) from 0.15 towards zero in permeabilized fibers of *vastus lateralis* (Pesta et al 2011). Although LEAK respiration increased slightly, the coupling efficiency 1-*L*/*E* increased with training. Both OXPHOS and ET capacities increased with training, but the more pronounced increase of *P* explains the decrease of *E*-*P* control efficiency (Figure 2e, f). This indicates that the limitation of *P* by the phosphorylation system was eliminated after strength and endurance training for 10 weeks.

The *E*-*P* control efficiency (N-pathway) is unchanged at 0.1 to 0.2 in permeabilized peripheral blood mononuclear cells (PBMCs) of a rat model of iron deficiency anemia (IDA), despite the surprising increase of citrate synthase activity and mitochondrial respiratory capacity in PBMCs from rats with IDA compared to controls (Fischer et al 2022). In contrast, the *E*-*P* control efficiency in liver homogenate declines from 0.4 in controls to 0.2 in IDA rats (Fischer et al 2022). Whereas N_E was unaffected by IDA, N_P increased in livers of IDA rats, indicating a specific activation of the phosphorylation system (Figure 2e, f).

In mitochondria isolated from liver of adult mice (4–5 months), the *E*-*P* control efficiency (S-pathway) is 0.6, but as low as zero in liver mitochondria of young (30–45 days) mice (Balmaceda et al 2024). While S_E was identical in liver mitochondria of adult and young mice, S_P and thus the capacity of the phosphorylation system was increased in liver mitochondria of young mice. No information is obtained on changes of mitochondrial density in the tissue from these studies of isolated mitochondria.

OXPHOS capacity (NS-pathway) is depressed in concentrated lysates of *Artemia franciscana* embryos in the state of diapause. This is mainly due to inhibition of the phosphorylation system as reflected by a high *E*-*P* control efficiency of 0.75, likely caused by long-chain acyl-CoA esters known to inhibit the adenine nucleotide translocator (Patil et al 2024). The *E*-*P* control efficiency decreases to 0.3 as the diapause extract with its inhibiting compound is diluted, reversing the depression of OXPHOS capacity (Figure 2e, f).

Inhibition of ET capacity (S-pathway, mouse brain homogenate) by 50 % exerts a small reduction of the mitochondrial membrane potential $\Delta\Psi_{mt}$ in the LEAK state without effect on *L*(n) in the absence of ADP or on *L*(Omy) when ATP synthase is inhibited (Krumschnabel et al 2014). Thus the *L*/*E* coupling control ratio is increased not due to an increase in *L* but a decrease in *E*. Under these conditions, the lower *E*-*L* coupling control efficiency (Figure 2 g, h) does not reflect dyscoupling.

4. Uncoupling and dyscoupling without change of *E*-*P* control efficiency

The neurotoxin and Complex I inhibitor MPP^+ exerts a strong impact on NS-linked ET capacity in permeabilized neuroblastoma cells and causes dyscoupling (decreased N-linked *P*-*L* coupling control), but the *E*-*P* control efficiency remains constant at c. 0.1 (Risiglione et al 2020). If dyscoupling and impairment of ET capacity (CI) were the only effects of MPP^+, the *E*-*P* control efficiency would decline to zero. Therefore, these results suggest a concomitant inhibition of the phosphorylation system.

Immobilization leads to atrophy of human skeletal muscle. Despite of a decline of *P*-*L* coupling control from 0.83 to 0.63 after 10 days of immobilization (N-pathway, permeabilized fibers measured at 25 °C), the *E*-*P* control efficiency (NS-pathway) remained constant at 0.22 since both *P* and *E* declined by 29 % (Hafen et al 2019). Daily

heat therapy, increasing muscle temperature by 4 °C to 40 °C prevents the decline of skeletal muscle respiratory capacity (Hafen et al 2019).

In horse skeletal muscle permeabilized fibers, *E-P* control efficiency is 0.15 independent of training level when measured at 37 °C (Votion et al 2012), but is close to zero and constant from physiological temperature (38 °C) to 44 °C, showing no limitation of respiration by the phosphorylation system (Davis et al 2020; Davis et al 2024). However, hyperthermia exerted dyscoupling, indicated by the decrease of coupling efficiency both in NADH- and succinate-linked pathways at 44 °C (Davis et al 2020). Under conditions of *P*=*E*, dyscoupling is not reflected by a change in the *E-P* control efficiency.

5. Coupling and mitochondrial pathways

Coupling control is investigated without changing the pathway state. A pathway state is obtained using specific combinations of fuel substrates and possibly inhibitors of branches of the electron transfer system. The additive effect of electron transfer pathways converging at the Q-junction (Komlódi et al 2021) leads to an increased ET capacity which may then exceed the capacity of the phosphorylation system, resulting in *E-P* control efficiency >0. Not only ET capacities vary between the separate or combined pathways with electron input converging at the Q-junction, but different numbers of coupling sites exert an effect on the *E-P* control efficiency (Gnaiger 2020).

The coupling sites are the respiratory Complexes CI, CIII, and CIV which pump protons towards the intermembrane space, generating the protonmotive force. Other respiratory Complexes, such as CII, CGpDH (mt-glycerophosphate dehydrogenase), CETFDH (electron-transferring flavoprotein dehydrogenase), are not involved in proton translocation, but reduce coenzyme Q, thus stimulating proton translocation by CIII and CIV. Pathways with a lower number of coupling sites are less likely to saturate the phosphorylation system capacity at identical rates of O_2 consumption. Therefore in a single pathway – such as the succinate (CII-linked) pathway – the *E-P* control efficiency is more likely to be zero. These details of OXPHOS analysis are not revealed in coupling control protocols with living cells (Zdrazilova et al 2022) but require the study of mitochondrial preparations.

Both LEAK and ET capacity can be considered as non-phosphorylating respiration. In the LEAK state, respiration is low and not coupled to ATP production by inhibition of ATP synthase by specific inhibitors or lack of the substrate ADP. In contrast, in the ET state, respiration is high after titration of a protonophore that precludes the ATP synthase from using the collapsed protonmotive force to synthesize ATP. That means, in the ET state the electron transfer system functions at its pathway-specific maximum capacity, while in the LEAK state, the ETS is stimulated only to the extent controlled by intrinsic uncoupling or extrinsic dyscoupling. Uncoupling can be related to different processes (Table 2 in Gnaiger et al 2020). Therefore care should be taken and clarification is required when using the terms uncoupling and non-phosphorylating respiration.

Abbreviations

E	electron transfer capacity	NS-pathway	NADH&succinate-linked pathway
ETS	electron transfer system		
L	LEAK respiration	*P*	OXPHOS capacity
N-pathway	NADH-linked pathway	S-pathway	succinate-linked pathway

References

Balmaceda V, Komlodi T, Szibor M, Gnaiger E, Moore AL, Fernandez-Vizarra E, Viscomi C (2024) The striking differences in the bioenergetics of brain and liver mitochondria are enhanced in mitochondrial disease. https://doi.org/10.1016/j.bbadis.2024.167033

Chance B, Williams GR (1955) Respiratory enzymes in oxidative phosphorylation: III. The steady state. https://doi.org/10.1016/S0021-9258(19)57191-5

Davis MS, Barrett MR, Bayly WM, Bolinger A (2024) Effect of selected fluorophores on equine skeletal muscle mitochondrial respiration. https://doi.org/10.26124/bec:2024-0002

Davis MS, Fulton MR, Popken AA (2020) Effect of hyperthermia and acidosis on equine skeletal muscle mitochondrial oxygen consumption. https://doi.org/10.1152/ajpregu.00177.2023

Doerrier C, Garcia-Souza LF, Krumschnabel G, Wohlfarter Y, Mészáros AT, Gnaiger E (2018) High-Resolution FluoRespirometry and OXPHOS protocols for human cells, permeabilized fibers from small biopsies of muscle, and isolated mitochondria. https://doi.org/10.1007/978-1-4939-7831-1_3

Estabrook RW (1967) Mitochondrial respiratory control and the polarographic measurement of ADP:O ratios. https://doi.org/10.1016/0076-6879(67)10010-4

Fischer C, Valente de Souza L, Komlódi T, Garcia-Souza LF, Volani C, Tymoszuk P, Demetz E, Seifert M, Auer K, Hilbe R, Brigo N, Petzer V, Asshoff M, Gnaiger E, Weiss G (2022) Mitochondrial respiration in response to iron deficiency anemia. Comparison of peripheral blood mononuclear cells and liver. https://doi.org/10.3390/metabo12030270

Gnaiger E (2020) Mitochondrial pathways and respiratory control. An introduction to OXPHOS analysis. 5th ed. https://doi.org/10.26124/bec:2020-0002

Gnaiger E et al - MitoEAGLE Task Group (2020) Mitochondrial physiology. https://doi.org/10.26124/bec:2020-0001.v1

Hafen PS, Abbott K, Bowden JA, Lopiano R, Hancock CR, Hyldahl RD (2019) Daily heat treatment maintains mitochondrial function and attenuates atrophy in human skeletal muscle subjected to immobilization. https://doi.org/10.1152/japplphysiol.01098.2018

Komlódi T, Cardoso LHD, Doerrier C, Moore AL, Rich PR, Gnaiger E (2021) Coupling and pathway control of coenzyme Q redox state and respiration in isolated mitochondria. https://doi.org/10.26124/bec:2021-0003

Krumschnabel G, Eigentler A, Fasching M, Gnaiger E (2014) Use of safranin for the assessment of mitochondrial membrane potential by high-resolution respirometry and fluorometry. https://doi.org/10.1016/B978-0-12-416618-9.00009-1

Lemieux H, Semsroth S, Antretter H, Höfer D, Gnaiger E (2011) Mitochondrial respiratory control and early defects of oxidative phosphorylation in the failing human heart. https://doi.org/10.1016/j.biocel.2011.08.008

Patil YN, Gnaiger E, Landry AP, Leno ZJ, Hand SC (2024) OXPHOS capacity is diminished and the phosphorylation system inhibited during diapause in an extremophile, embryos of *Artemia franciscana*. https://doi.org/10.1242/jeb.245828

Pesta D, Hoppel F, Macek C, Messner H, Faulhaber M, Kobel C, Parson W, Burtscher M, Schocke M, Gnaiger E (2011) Similar qualitative and quantitative changes of mitochondrial respiration following strength and endurance training in normoxia and hypoxia in sedentary humans. https://doi.org/10.1152/ajpregu.00285.2011

Risiglione P, Leggio L, Cubisino SAM, Reina S, Paternò G, Marchetti B, Magrì A, Iraci N, Messina A (2020) High-resolution respirometry reveals MPP^+ mitochondrial toxicity mechanism in a cellular model of parkinson's disease. https://doi.org/10.3390/ijms21217809

Steinlechner-Maran R, Eberl T, Kunc M, Margreiter R, Gnaiger E (1996) Oxygen dependence of respiration in coupled and uncoupled endothelial cells. https://doi.org/10.1152/ajpcell.1996.271.6.C2053

Votion DM, Gnaiger E, Lemieux H, Mouithys-Mickalad A, Serteyn D (2012) Physical fitness and mitochondrial respiratory capacity in horse skeletal muscle. https://doi.org/10.1371/journal.pone.0034890

Zdrazilova L, Hansikova H, Gnaiger E (2022) Comparable respiratory activity in attached and suspended human fibroblasts. https://doi.org/10.1371/journal.pone.0264496